sustainability

MDPI

Article

Technical and Economic Analysis of Solar PV/Diesel Generator Smart Hybrid Power Plant Using Different Battery Storage Technologies for SRM IST, Delhi-NCR Campus

Shilpa Sambhi [1], Himanshu Sharma [1,*], Vikas Bhadoria [2], Pankaj Kumar [1], Ravi Chaurasia [1], Georgios Fotis [3,*] and Vasiliki Vita [3]

[1] Department of Electrical and Electronics Engineering, SRM Institute of Science and Technology, Delhi-NCR Campus, Ghaziabad 201204, Uttar Pradesh, India
[2] Industry Integration Cell, Shri Vishwakarma Skill University, Palwal 121102, India
[3] Department of Electrical and Electronic Engineering Educators, School of Pedagogical and Technological Education, 14121 Athens, Greece
* Correspondence: himanshuresearch58@gmail.com (H.S.); gfotis@gmail.com (G.F.)

Abstract: This paper presents atechnical and economic analysis of the proposed solar PV/diesel generator smart hybrid power plant for a part of SRM IST, Delhi-NCR campus. The analysis was performed using five battery storage technologies: lead-acid, lithium-ion, vanadium flow, zinc bromide and nickel-iron. The analysis also used the HOMER Pro software. The analysis was conducted to assess performance parameters such as initial cost, simple payback period, return on investment, energy produced, renewable penetration and emission of air pollutants. The optimal solution was obtained as SPP(200 kW)/DG(82 kW)/ZB(2000 kWh), with cycle charging dispatch strategy. The initial cost of this configuration is estimated to be USD163,445, and the operating cost is USD534 per year. The net present cost is estimated to be USD170,348, and the estimated cost of energy with this configuration has been obtained as USD0.090 per kWh. It is estimated that with this optimal solution, the diesel generator may consume only 110 L/year of diesel, which is the minimum of all configurations. Sensitivity analysis was performed between the size of the solar PV array and the size of the battery, along with variations in the battery's nominal capacity and renewable fraction.

Keywords: technical–economic analysis; levelized cost of energy; net present cost; hybrid power plant; battery technology

Citation: Sambhi, S.; Sharma, H.; Bhadoria, V.; Kumar, P.; Chaurasia, R.; Fotis, G.; Vita, V. Technical and Economic Analysis of Solar PV/Diesel Generator Smart Hybrid Power Plant Using Different Battery Storage Technologies for SRM IST, Delhi-NCR Campus. *Sustainability* **2023**, *15*, 3666. https://doi.org/10.3390/su15043666

Academic Editor: Lin Hu

Received: 14 December 2022
Revised: 2 February 2023
Accepted: 15 February 2023
Published: 16 February 2023

1. Introduction

The increasing demand for electricity in developing countries such as India due to upcoming automation industries, smart cities and smart devices has motivated a shift in electricity generation from fossil fuels to renewable energy sources (RES). Another reason to shift towards RES is the increasing emission of greenhouse gases (GHG) such as carbon dioxide (CO_2) in the environment. In 2022, global GHG emissions increased by 4.8% as the demand for electricity generation has increased. Hence, the demand for fossil fuels has also increased [1]. India accounts for 7.32% of global emissions [2]. India has committed to reducing GHG emissions by 45% by 2030 and achieving around 50% electricity generation from non-fossil fuel-based energy resources by 2030 [3]. The Kyoto protocol aims to reduce the emission of GHG, which include CO_2, methane, nitrous oxide and fluorinated gases [4]. Electricity generation using RES may help reduce fossil fuel dependency and GHG emissions. Rural areas may also benefit from generating electricity using locally available renewable sources and nonconventional sources of energy [5]. Commissioning a decentralized stand-alone smart hybrid power plant (HPP) near the load center decreases the distribution and transmission losses related to the primary grid [6].

Currently, India has installed 163 GW of RES, which includes 41.2 GW of wind energy, 59.34 GW of solar energy and the remainder from waste-to-energy, biomass and

hydropower [7]. This means that RES, including hydro, account for 40.4% of India's total energy capacity [8]. The installed solar capacity is 60,814 MW, which constitutes 14.9% of electricity generation using RES [8]. India experiences more than 300 sunny days per year, so stakeholders are more attracted to power generation using solar energy [2]. It is estimated that the cost of energy reduces by a significant amount when electricity is generated using RES [9]. Some of India's solar power plants (SPP) are in Rajasthan, Karnataka, Andhra Pradesh, Madhya Pradesh and Tamil Nadu [10]. The world's largest SPP has been installed in Bhadla in Rajasthan, India, with a capacity of 2245 MW [11].

Solar energy is intermittent and dependent on weather conditions. Depending on the weather forecast, electricity generation through SPPs is planned [12]. Solar energy is unavailable during the rainy season and night hours, so the SPP cannot generate electricity. The load demand can be smoothly fulfilled by combining other electricity generation technologies, such as wind energy, energy storage systems, diesel generators, biomass and hydro, with SPPs. The improvement in renewable penetration and reduction in GHG emissions can be observed by commissioning smart HPPs [13]. It is imperative to understand that the planning and optimal sizing of a stand-alone HPP is challenging from a techno-economic point of view [14,15]. The reason is that if the system is oversized, then it may increase the cost of the system, and excess energy may be generated, while if the system is undersized, then it may fail to meet the load demand. The excess energy generated can be stored in an appropriate energy storage system such as a battery [16]. In that case, the energy stored in the battery storage system (BSS) is utilized to serve the load or meet the peak load demand. For that reason, it is necessary to choose a reliable BSS to enhance the stand-alone HPP's reliability and cost-effectiveness [17]. The recent advancement in BSS technology has allowed it to become an appropriate choice based on feasibility and techno-economic viability. As a result, it can serve commercial or residential loads effectively. A region's climatic and other weather conditions affect the operation and performance of implemented BSS technology.

HPPs' most popular BSS technology is the lead-acid (LA) battery. It is a rechargeable battery, which offers operational safety, less capital and lower implementation cost. Apart from industrial and automotive applications, the LA battery is efficiently used for storing excess energy generated by a smart HPP [18]. This battery technology has moderate round-trip efficiency and low cost [19,20]. The features of the LA battery are as follows: specific energy of 30–50 Wh/kg, specific power of 75–300 W/kg, round-trip efficiency of 70–80%, service life of 5–15 years and self-discharge rate of 0.1–0.3% [21]. Recently, the lithium-ion (LI) battery has become popular for the following reasons: better storage capacity, better safety and less maintenance cost than the LA battery [17]. LI battery technology has high energy and power density, making it suitable as an energy storage system in HPPs [22]. The features of the LI battery are as follows: specific energy of 75–250 Wh/kg, specific power of 150–315 W/kg, round-trip efficiency of 85–95%, service life of 5–15 years and self-discharge rate of 0.1–0.3% [23]. This battery technology possesses high specific energy and high specific power, making it suitable for lightweight applications [23]. Many other advanced BSS technologies are currently available, which can bear high temperatures and harsh weather conditions. Such advanced BSS technologies are possible through thin-plate technology, pure lead technology and distinctive manufacturing methods [24]. Vanadium flow (VF) batteries and zinc bromide (ZB) flow batteries are examples of advanced BSSs. Flow battery features are as follows: specific energy of 10–35 Wh/kg, specific power of 100–166 W/kg, round-trip efficiency of 65–85%, service life of 15 years and self-discharge rate of 0% [21]. Therefore, the flow battery provides higher energy capacity than the LA and LI batteries. Even if the flow battery is fully discharged or not charged for a long time, the life of the flow battery is not compromised. It can be charged again to its total capacity. This is a benefit of using a flow battery in stand-alone smart HPPs [24]. For many years, nickel-based batteries have been used in many applications for storing energy, but recently, the nickel-iron (NI) battery is gaining popularity in off-grid solar power plants. NI batteries have high robustness, high resistance against overcharge–discharge cycles and tolerance

against high temperatures. This battery has a lifespan of 2000 to 3000 cycles. Though the NI battery has high manufacturing cost and a high rate of self-discharge, their long durability can save replacement cost compared to other battery technologies [25,26].

In the present study, the impact of LA battery, LI battery, VF battery, ZB battery and NI battery technologies were studied at SRM IST, Delhi-NCR educational campus. A comprehensive overview of smart HPPs involving different BSS technologies is presented in Table 1. Researchers have used different parameters to evaluate the performance of smart HPPs. These parameters have been related to cost (e.g., cost of energy, net present cost, operating cost), battery performance parameters (e.g., annual throughput, expected lifespan), GHG emissions, load served and renewable fraction [17].

Table 1. Overview of HPPs using different BSS technologies.

HPP Architecture	Location	On-Grid/Off-Grid	BSS Technology	COE (USD/kWh)	Ref
SPV/BG/battery	Odisha, India	Off-grid	LA, LI, NI battery	0.219–0.711	[27]
PV/wind/battery	India	Off-grid	LI battery	0.470	[28]
PV	Yucatan, Mexico	Off-grid	LA, LI battery and absorbent glass material	0.14	[29]
PV/wind/DG/battery	Peelee Island	Off-grid	LI battery	0.343	[14]
PV/wind/micro gas turbine	Australia	Off-grid	LA, LI, VF battery	0.126–0.187	[30]
PV/DG/battery	Andaman and Nicobar Islands, India	Off-grid	LA, LI, VF, ZB battery	0.155–0.167	[17]
PV/DG/battery	Modinagar, India	Off-grid	LI battery	0.34	[11]
PV/DG/battery	Shimla, India	Off-grid	LI battery	0.371	[31]
PV/wind/battery	Morocco	Off-grid	Surrette 6CS25P battery	0.171–0.32	[32]
PV/DG/battery	Tamilnadu, India	On-grid/Off-grid	LA battery	1.22–1.60	[33]
Wind/battery	Italy	Off-grid	LiFePO4, nickelmanganese cobalt oxide and flywheel	0.09	[34]
PV/biomass gasifier/battery	Himalaya, India	Off-grid	LI battery	0.185	[35]

In this research article, one of the academic buildings of SRM IST, Delhi-NCR campus, was considered for techno-economic analysis. Its geographical location is 28.8377° N and 77.5826° E. The selected site is marked on the map provided as Figure 1 [36]. Delhi-NCR experiences almost 300 sunny days per year but has a low potential for generating wind or hydro energy [11], but the minimum temperature during the winter season in Delhi-NCR drops down to around 1 °C for only two to three days in a year [37]. The campus aims to provide a green environment, which is in line with the Kyoto Protocol followed by the Indian government. For this purpose, it is proposed to commission a stand-alone SPP for a part of the selected academic building on the campus. The selected part of the building comprises 15 classrooms. While balancing the technical and economic factors, the design of the smart HPP is also optimized. This paper is organized as follows: the introduction to the work is given in Section 1; in Section 2, the motivation of the work is provided; and the methodology and load profile are provided in Section 3. The components of the proposed smart HPP are discussed in Section 4, modeling of the HPP is provided in Section 5, and Section 6 provides the results and discussions. Sensitivity analysis is given in Section 7, Section 8 provides the energy balance, and Section 9 draws the conclusions.

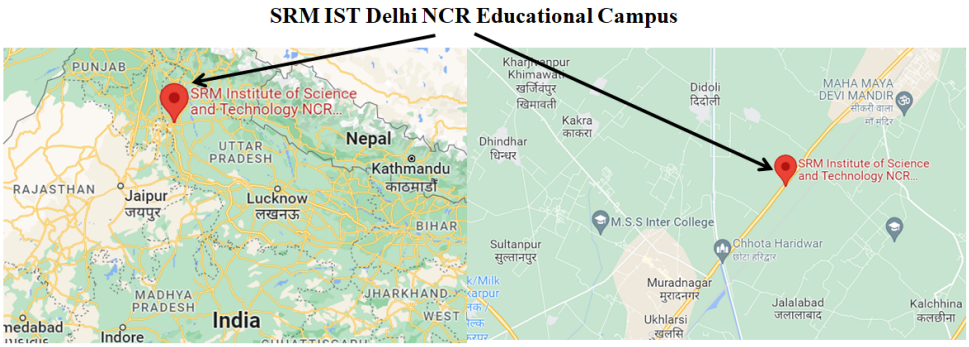

Figure 1. Map showing SRM IST, Delhi-NCR campus.

2. Motivation

India is situated north of the equator between latitudes 8°4′ N and 37°6′ N and longitudes 68°7′ E and 97°25′ E [38]. India receives average yearly solar radiation in the range of 3.0 to 6.5 kWh/m^2-day [39], and the average yearly ambient temperature of the country lies between 25 °C and 27 °C [40]. Approximately 5000 trillion kWh per year of energy is incident over Indian land [41]. The government of India has been working on various policies to promote electricity generation through solar energy, including standards for commissioning solar photo-voltaic systems, guidelines for rooftop solar and providing loans from agencies [42,43]. Presently, the selected site receives electricity from the primary grid, where electricity is generated from coal. A DG is used as a captive source of power generation.

The benefits of commissioning an SPP on the campus are as follows: (i) dependence on the primary grid for electricity supply is reduced, (ii) the cost of energy is reduced, (iii) usage of the diesel generator (DG) is reduced, and (iv) low emission of GHG due to less use of the DG. The SPP is proposed to be integrated with a BSS and DG to meet the peak demand or load requirement when the SPP does not generate electricity during night hours. Therefore, choosing suitable BSS technology to store excess energy generated from the SPP during the daytime is essential.

3. Methodology and Load Profile

The impact of different BSS technologies integrated with the proposed smart HPP was analyzed using HOMER software. The National Renewable Energy Laboratory, USA, developed this software. It also provides a platform for technical and economic analysis of the proposed HPP [44]. Figure 2 presents the block diagram of the HOMER Pro software to understand the outline of the work conducted in this study. The input information for HOMER is the geographical coordinates of the selected site, climatic conditions, fuel price and technical data of the components of the smart HPP. The analysis was performed with different BSS technologies to obtain the optimal solution for the considered load, which is to be served by the proposed HPP. The parameters considered for evaluation were NPC, COE, initial cost, renewable fraction, consumption of diesel and DG operation hours. Sensitivity analysis was performed to study the impact of the size of the SPP and BSS, with sensitivity variables taken as nominal battery capacity and renewable fraction.

The estimated load of 15 classrooms in a building at the SRM-IST campus is provided in Table 2. A typical classroom consists of LED lights, ceiling fans, an air conditioner, an LCD projector, a PA system (microphone and speakers), a computer system and plug points. The primary demand of the load occurs during the daytime due to the schedule of classes. The average daily usage of one classroom is 6 h, with an average energy consumption of approximately 400 kWh per day. The 24 h load profile of 15 classrooms is shown in Figure 3. The hourly load profile of 15 classrooms was taken as the input of the electric load component of the HOMER Pro software. The weekday and weekend load profiles were considered the same. The yearly load profile of 15 classrooms is shown in Figure 4. In

the present study, different BSS technologies were assessed to choose the optimal storage system for the excess energy produced by the SPP system.

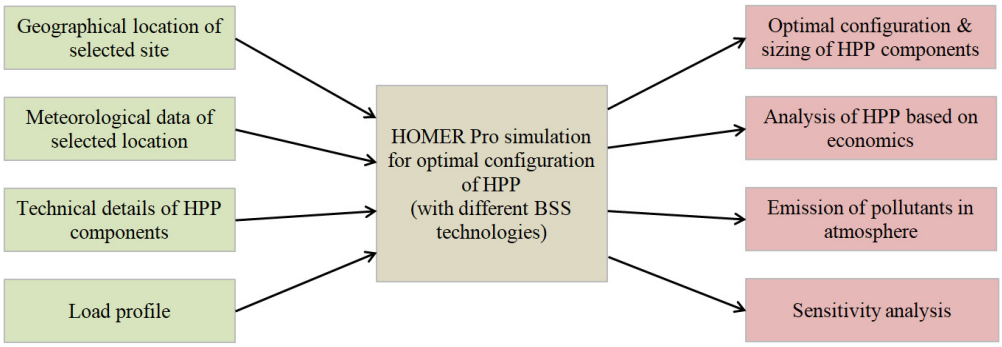

Figure 2. Block diagram representing the flow chart of HOMER software.

Table 2. Load estimation of 15 classrooms at the selected site.

Sr. No.	Load	Power (Watts)	Quantity	Usage (Hours)	Total Load (Wh)
1	LED light	24	6	6	864
2	Ceiling fans	20	5	6	600
3	Air conditioner (1.5 ton)	1500	2	6	18,000
4	LCD projector	280	1	6	1680
5	PA system (microphone and speakers)	800	1	6	4800
6	Computer system	100	1	6	600
7	Mobile charging point	3	2	6	36
	The total load for one classroom				26,580 Wh/day
	The total load for 15 classrooms				398.7 kWh/day (~400 kWh/day)

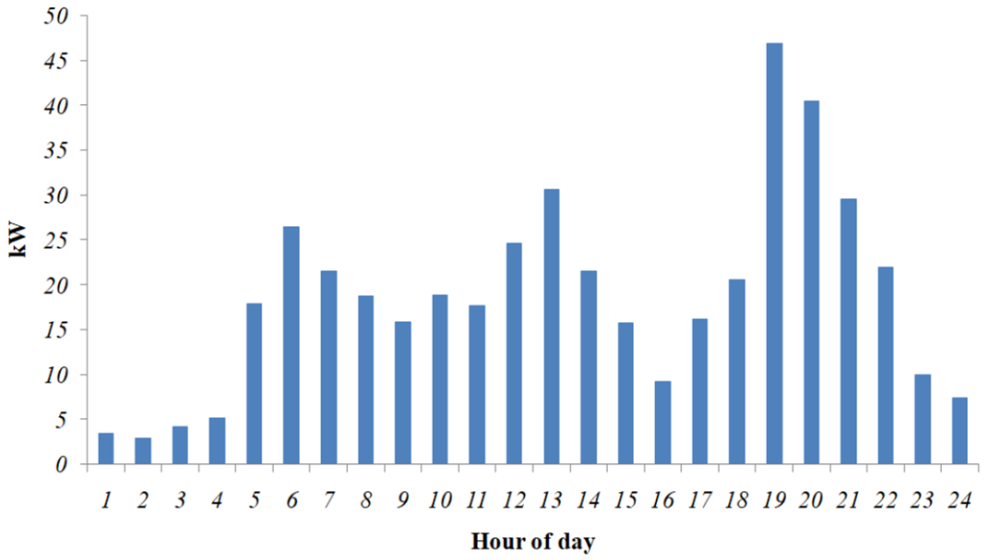

Figure 3. 24 h load profile for 15 classrooms in a building at SRM-IST, Delhi-NCR campus.

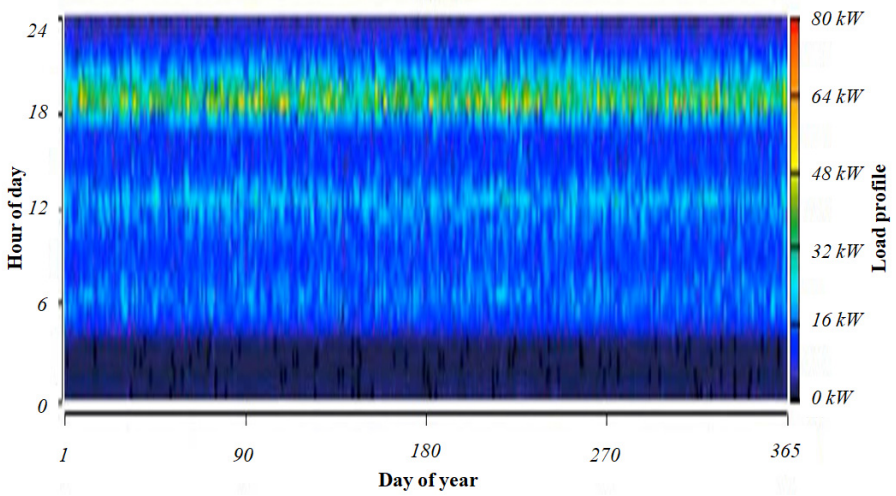

Figure 4. Yearly load profile of 15 classrooms at the SRM IST campus.

4. Components of Smart HPP

It is proposed that the smart HPP consists of an SPP, BSS and DG. Before commissioning the HPP, it is worthwhile to estimate the performance of all the components of the HPP based on the availability of renewable and nonrenewable resources. In this case, the renewable source is solar energy, and the nonrenewable source is diesel used as fuel in the DG. After fulfilling the demand of the load, the excess energy generated, either by the SPP or DG, may be stored in the BSS. The energy stored in the BSS can be utilized to serve the load during peak demand, and the DG provides captive power generation when the SPP, BSS or both fail to serve the load.

4.1. SPP Assessment

The solar radiation incident on the solar panel and the ambient temperature affect electricity generation from the SPP system. Figure 5 presents the average monthly daylight hours, average monthly ambient temperature and Earth skin temperature. Total solar radiation received on the Earth's horizontal surface is known as ALLSKY INSOL [45]. The ALLSKY INSOL and clearness index of the selected location were taken from the HOMER Pro software and are presented in Figure 6. Due to dust particles and moisture content present in the atmosphere, solar radiation received on the Earth's surface is scattered, known as diffuse horizontal irradiance (DIFF) [46]. The radiation received on the Earth's surface measured at a specific location is known as direct normal radiance (DNR). This component does not include scattered radiation due to atmospheric components [47]. Therefore, DNR depends on the selected location's weather conditions, the time of day and time of year. The information related to ALLSKY INSOL, DIFF and DNR was taken from the NASA-PDAV tool and is shown in Figure 7 for the selected site [48].

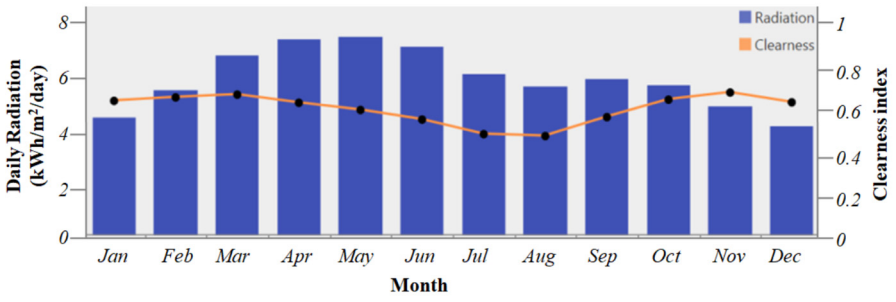

Figure 5. Average monthly ambient temperature, Earth skin temperature and daylight hours at SRM IST, Delhi-NCR campus.

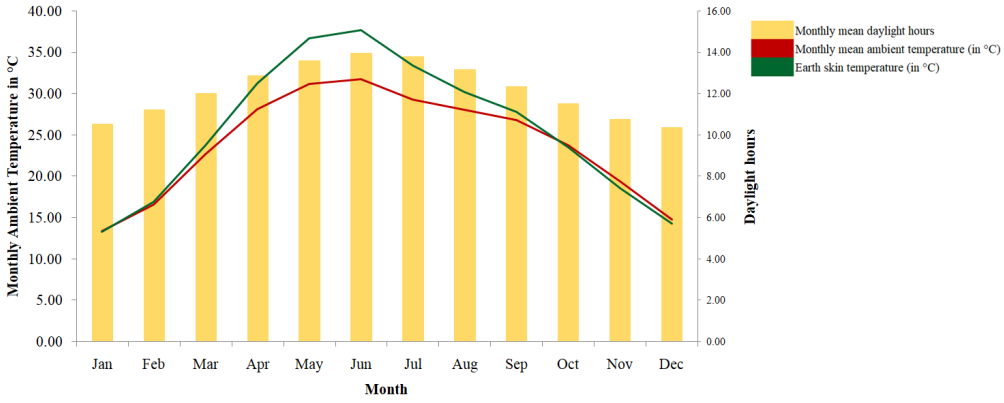

Figure 6. Solar radiation (ALLSKY INSOL) and clearness index of the SRM-IST campus.

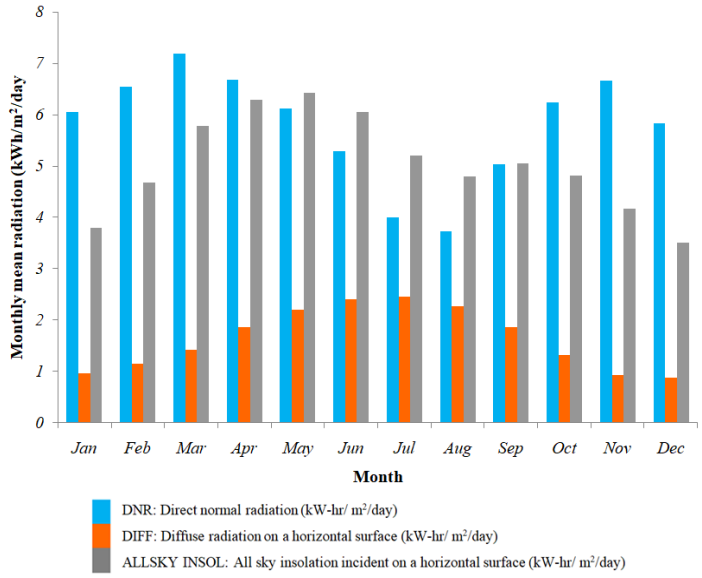

Figure 7. ALLSKY INSOL, DIFF and DNR of the solar radiation for the SRM-IST campus.

The SPP system generates electricity in DC. Because the load is AC in nature, it must be converted to AC before serving it. For the proposed configuration, the polycrystalline PV array and its technical details are provided in Table 2. HOMER Pro applies Equation (1) [49] to calculate the solar array output power.

$$P_{output} = Y_{pv} f_{pv} \left(\frac{G_T}{G_{T,STC}} \right) \left[1 + \alpha_p (T_c - T_{c,STC}) \right] \quad (1)$$

where, under standard test conditions, Y_{PV} is the output power in kW from the solar array; f_{PV} is the derating factor in % of the solar array; G_T is the solar radiation in kW/m^2, which is incident on the PV array; $G_{T,STC}$ (1 kW/m^2) is the incident radiation from the sun; α_P is the power temperature coefficient in % per °C; T_c is the temperature in °C of the PV cell in the current time step; and $T_{c,STC}$ is the temperature of the PV cell in °C. Equation (1) can be simplified by neglecting the effect of temperature on the solar array, as shown in Equation (2). In this case, HOMER assumes α_P to be zero [50]. The technical details of the solar PV panel considered in this study are provided in Table 3.

$$P_{PV} = Y_{PV} f_{PV} \left(\frac{G_T}{G_{T,STC}} \right) \quad (2)$$

Table 3. Technical details of the solar PV panel.

Description	Value
Type of panel	Flat plate
Name (abbreviation)	PV
Rated capacity (kWp)	1
Capital cost (USD/kW)	470
Replacement cost (USD/kW)	470
O&M cost (USD/year)	2.66
Lifetime (years)	25
Derating factor (% assumed)	80
Temperature coefficient (per °C)	−0.5
Nominal operating cell temperature (°C)	47
Efficiency (%)	0.13

4.2. DG Assessment

A DG was made part of the smart HPP as a source of captive power generation. There are chances that the SPP will fail to generate enough electricity to serve the load demand. It could happen because of the following reasons: (1) the weather is cloudy or rainy, and (2) during night hours, the SPP does not receive sunlight to generate electricity. In such a case, the DG operates to serve the load. The diesel-based generator was considered because diesel as a fuel is readily available to operate the DG. Depending on the rated capacity of the DG and the electrical energy output from the DG, fuel consumption in the DG is governed by Equation (3) [51,52].

$$C_{DG} = f_1 Y_{DG} + f_2 P_{DG} \tag{3}$$

where C_{DG} is fuel consumption in liters, f_1 is the coefficient of the fuel curve in L/h/kW, Y_{DG} is the rated capacity of the DG in kW, f_2 is the fuel curve slope in L/h/kW and P_{DG} is the generated power of the DG in kW. Depending on the DG's electricity generated, the DG's efficiency is calculated using Equation (4) [52,53].

$$\int \eta_{DG} = \frac{3.6 P_{DG}}{C_{DG} \rho_{DG} H_{LD}} \tag{4}$$

where ρ_{DG} is the density of the diesel fuel (kg/m^3) and H_{LD} is the lower heating response of the diesel fuel (MJ/kg). The technical details of the diesel generator considered in this study are provided in Table 4.

Table 4. Technical details of the diesel generator.

Description	Value
Fuel	Diesel
Capital cost (USD/kW)	665
Replacement cost (USD/kW)	535
O&M cost (USD/h)	0.027
Fuel price (USD/L)	1.14
Lifetime (hours)	15,000
CO (g/L/fuel)	16.5
Unburned HC (g/L fuel)	0.72
Particulates (g/L fuel)	0.1
Fuel sulfur to PM (%)	2.2
NOX (g/L fuel)	15.5

5. Modeling of Smart HPP

In this study, based on the requirement of 15 classrooms in an academic building at the SRM IST campus, the SPP/BSS/DG hybrid configuration was simulated to determine the

optimal configuration to serve the load. The smart HPP, shown in Figure 8, was operated with five different BSS technologies using HOMER software to analyze the technical and economic parameters of the selected load.

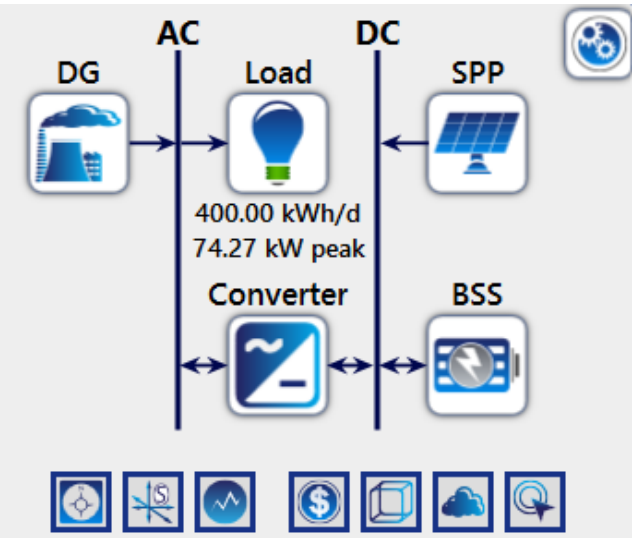

Figure 8. Proposed smart HPP configuration using different BSS technologies.

5.1. Description of Smart HPP Components

The proposed off-grid smart HPP consists of (1) an SPP, (2) a DG, (3) a converter, and (4) a BSS–LA battery, LI battery, VF battery, ZB battery and NI battery. For optimal configuration, HOMER software considers capital cost, replacement cost, operation and maintenance (O&M) cost and a lifetime to simulate the system, as presented in Table 5. The technical details of the SPP and DG are provided in Tables 3 and 4. The power generated by the SPP was calculated using Equation (1) by HOMER. The combination of the SPP and BSS is a lowly reliable hybrid system, as power generation from the SPP depends on weather conditions. After serving the load, the BSS is charged from excess power generated by the SPP. Therefore, the DG is also employed with the SPP and BSS to enhance the reliability of the smart HPP. HOMER has plotted a fuel curve to show diesel consumption, as shown in Figure 9. The characteristics curve about the rated capacity of 50 kW DG was obtained, with a slope of 0.236 L/h/kW and an intercept coefficient of 3.33 L/h [54]. The efficiency curve for the DG output plotted between zero, and the rated output is shown in Figure 10. The diesel used as fuel constitutes 0.4% sulphur content, 88% carbon content, 43.2 MJ/kg of lower heating value and density of 820 kg/m^3. The DG's emissions per liter of fuel consumption are 16.5 g of CO, 0.72 g of unburned hydrocarbon, 0.1 g of particulate matter and 15.5 g of NOx [54].

Table 5. Financial metrics and life span of HPP components.

Components	Capital Cost (USD)	Replacement Cost (USD)	O&M Cost (USD)	Life Span
SPP	470 per kW	470 per kW	2.66 per year	25 years
DG	665 per kW	535 per kW	0.027 per op. h	15,000 h
Converter	195 per kW	195 per kW	4 per year	15 years
LA battery	135 per kWh	108 per kWh	1.33 per year	5 years
LI battery	500 per kWh	455 per kWh	0	10 years
VF battery	535 per kWh	465 per kWh	0	25 years
ZB battery	800 per kWh	735 per kWh	0	25 years
NI battery	106 per kWh	98 per kWh	2.12	25 years

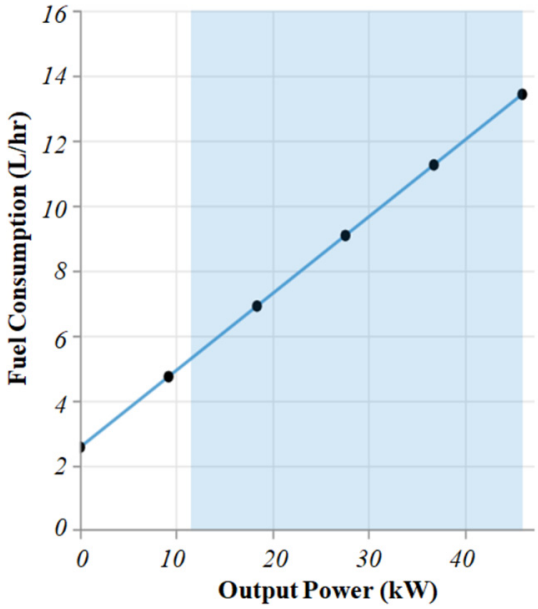

Figure 9. Fuel curve of the diesel generator.

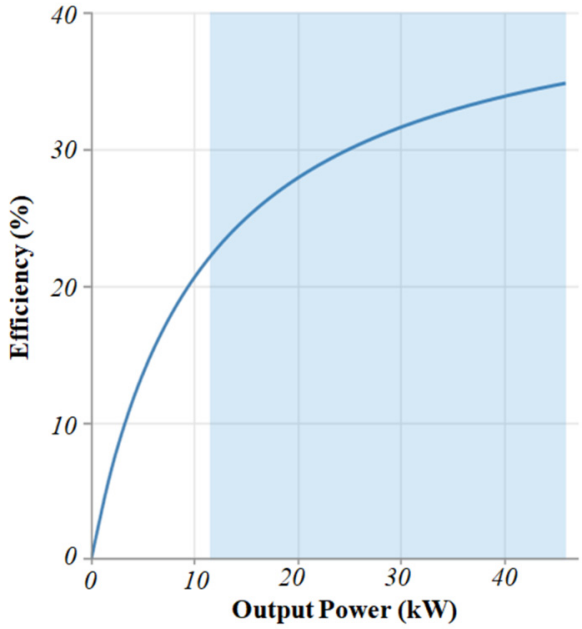

Figure 10. Efficiency curve of the diesel generator.

HOMER software has two optimization algorithms: original grid search algorithm and HOMER optimizer. These are derivative-free algorithms to search for the least-cost system. The optimization results obtained are sorted by net present cost. The maximum simulations per optimization are automatically taken by HOMER optimizer. This prevents the optimization from running forever, and it converges after a finite number of simulations.

The power generated by the SPP and provided by the BSS is DC power. This DC power was converted to AC power using a converter before serving the load, as shown in Figure 8. If the DG is operating, then AC power is converted by this converter to DC

power to charge the BSS. The size of the converter depends on the peak demand [55]. The power provided by the converter is expressed as Equation (5) [56].

$$P_{Con} = \frac{P_{Peak}}{\eta_{Con}} \tag{5}$$

where P_{Con} is the power rating of the converter in kW, P_{Peak} is the peak load demand of the system in kW and η_{Con} is the conversion efficiency in % of the converter. For the current study, the conversion efficiency of the converter is taken as 90% [57].

For any HPP, it is essential to have an energy storage system for the following reasons: (1) due to the intermittent nature of sunlight, the SPP may not be able to serve the load during some interval of time—in such a case the energy stored in the BSS serves the load; and (2) during peak load, the BSS helps to maintain constant voltage by providing stored energy to the load. The technical parameters of selected BSS technologies used in the current study are presented in Table 6 [13,17]. The initial state of charge (SOC) for each BSS was taken as 100%, while the minimum SOC for each BSS was taken as 20% [57]. HOMER software utilizes themathematical expressions provided in Equations (6) and (7) to calculate the charging and discharging power of the battery bank [17,58].

$$P_{bat,c-\max} = \frac{kQ_{start}e^{-k\Delta t} + Q_{total}kc_r(1 - e^{-k\Delta t})}{1 - e^{-k\Delta t} + c_r(k\Delta t - 1 + e^{-k\Delta t})} \tag{6}$$

$$P_{bat,d-\max} = \frac{-kc_rQ_{rated} + kQ_{start}e^{-k\Delta t} + Q_{total}kc_r(1 - e^{-k\Delta t})}{1 - e^{-k\Delta t} + c_r(k\Delta t - 1 + e^{-k\Delta t})} \tag{7}$$

where $P_{bat,c\text{-}max}$ is the maximum charging power in kW of the battery bank, k is the storage rate constant in h^{-1}, Q_{start} is the available stored energy at the start of the time step in kWh, Δt is the time step span in hours, Q_{total} is the total energy stored at the start of the time step in kWh, C_r is the ratio of the storage capacity, $P_{bat,d\text{-}max}$ is the discharging power in kW of the battery bank and Q_{rated} is the rated capacity of the battery bank in kWh.

Table 6. Technical parameters of selected BSS technologies.

Characteristics Parameters	LA Battery	LI Battery	VF Battery	ZB Battery	NI Battery
Nominal voltage (V)	12	6	50	600	1.2
Nominal capacity (kWh)	1	1	5	1000	0.12
Maximum capacity (Ah)	83.4	167	150	1670	100
Round-trip efficiency (%)	80	90	80	90	85
Maximum charge current (A)	16.7	167	132	1670	50
Maximum discharge current (A)	24.3	500	200	5000	50

5.2. Dispatch Control Strategy

The proposed smart HPP was operated with two types of dispatch control strategies: load following (LF) and cycle charging (CC). These strategies control the operation of the components generating energy and the energy storage system in the HPP. Such control strategies can be implemented using suitable controllers such as programmable logic controllers or microcontrollers [59]. In the CC strategy, whenever the DG operates, it operates at full output power. The excess energy produced serves the low-priority loads such as charging of the BSS or serving the deferrable load [11]. In the LF strategy, whenever the DG operates, it generates enough power to serve the primary load. Renewable energy sources serve the lower-priority loads such as charging of the BSS or serving the deferrable load. If it is economically advantageous, the DG may generate excess power and sell this to the grid [14]. Suppose that the power generated (by the SPP or DG) or power delivered (by the BSS) is P in kW and load demand is P_L in kW. In that case, there are the following three cases in the LF strategy [60,61]:

1. P = P_L. In this case, only the SPP is operated to serve the primary load. The BSS is not charged, and the DG is not operated.

2. $P > P_L$. In this case, after serving the primary load, the excess power charges the BSS, but the DG is not operated.
3. $P < P_L$. In this case, the SOC of the battery is compared with the minimum value of SOC (SOC_{min}) to decide the operation of the DG. Based on the SOC status, the following two cases may arise:
   (a) If $SOC = SOC_{min}$, the DG operates to generate only deficit energy between the SPP and primary load. During operation, if minimum DG loading is greater than deficit power, excess energy is utilized to charge the BSS.
   (b) If $SOC > SOC_{min}$, the cost of discharging BSS energy is compared with the cost of energy generated from the DG. The component with the minimum cost operates to serve the primary load connected to the smart HPP.

5.3. Economic Modelling of Smart HPP

The optimal configuration of an off-grid smart HPP provided by HOMER software is based on the net present cost (NPC) of the HPP and cost of energy (COE) of power generated from the HPP. The NPC of the HPP is evaluated using Equation (8) [62,63].

$$NPC = \frac{C_{ann}}{CRF(r,t)} \tag{8}$$

where C_{ann} is the total annual cost of the HPP in USD/year, r is the annual rate of interest in %, t is time in years and $CRF(r, t)$ is the capital recovery factor which is a function of r and t. $CRF(r, t)$ and r can be calculated using Equations (9) and (10) [17].

$$CRF(r,t) = \frac{r(r+1)^t}{(r+1)^t - 1} \tag{9}$$

$$r = \frac{r' - f}{1+f} \tag{10}$$

where f is yearly inflation rate of HPP in %. In the current study, r is taken as 10% and f as 2%. The COE produced by the HPP was evaluated as the ratio of the total annual cost of the HPP to the annual energy supplied to the load, E_n, in kWh, excluding excess energy, as given in Equation (11) [17,62]. The total annual cost of the HPP was obtained using Equation (12), where C_{CC} is the annual capital cost in USD, C_{RC} is annual replacement cost in USD and C_{OM} is annual O&M cost in USD [17].

$$COE = \frac{C_{an}}{E_n} \tag{11}$$

$$C_{an} = C_{CC} + C_{RC} + C_{OM} \tag{12}$$

6. Results and Discussion

HOMER software simulated an off-grid smart HPP with an SPP, DG and BSS as its components. Five different BSS technologies—LI battery, LA battery, VF battery, ZB battery and NI battery—were considered to serve the selected load. The optimized results obtained are presented in Table 7. The impact of selected BSS technologies was compared with a reference system while considering economic parameters such as NPC (USD), COE (USD/kWh), return on investment (%), simple payback period (years), emission of pollutants (kg/year), renewable penetration (%) and electrical energy generation (kWh). This analysis supported selection of a technically and economically feasible smart HPP configuration. Further, the effect of variations in sizing of the SPP and BSS was analyzed by considering sensitivity variables such as nominal battery capacity and renewable fraction. Finally, the energy balance of the smart HPP was analyzed for 24 h of operation.

Table 7. Optimal HPP configuration for selected load.

HPP Architecture	SPP (kW)	DG (kW)	Battery (kWh)	Converter (kW)	Dispatch Strategy	NPC (USD)	COE (USD/kWh)	Operating Cost (USD/Year)	Initial Cost (USD)	Renewable Fraction (%)	Fuel (L/Year)
SPP/DG/LA	200	82	524	64	LF	411,676	0.218	13,918	231,746	96	2460
SPP/DG/LI	200	82	320	64	LF	499,671	0.265	13,827	320,929	94	3103
SPP/DG/VF	200	82	6514	56	LF	356,427	0.189	7090	264,769	95	2812
SPP/DG/ZB	200	82	2000	68	CC	170,348	0.090	534	163,445	99	110
SPP/DG/NI	200	82	292	64	LF	504,112	0.267	6614	418,615	94	3302
DG	-	82	-	-	LF	1,711,763	0.907	128,194	54,530	0	74,128

6.1. Optimum Solution Analysis

The simulations were performed by HOMER software for the proposed off-grid smart HPP to find the feasible configuration for the selected load. In the proposed HPP, a solar PV array of 200 kW and DG of 82 kW were taken. The capacity of the solar PV array was chosen based on the area available for installing solar panels, and depending on the load, the capacity of the DG was chosen. The combination of the SPP and DG was simulated, along with different BSS technologies. HOMER simulates the objective function of minimizing the NPC of the HPP. As the capacity of the SPP and DG was fixed, HOMER software carried out optimal sizing of the BSS. The COE of the HPP decreases with a decrease in NPC, as can be seen Equations (8)–(11). The HPP configurations simulated were SPP/DG/LA, SPP/DG/LI, SPP/DG/VF, SPP/DG/ZB, SPP/DG/NI and DG only. A comparison was made between these six configurations with respect to NPC, as shown in Figure 11. It was found that the SPP/DG/ZB configuration has the lowest NPC of USD170,348. In addition, a comparison of COE was made among these six configurations, as shown in Figure 12, and it was found that SPP/DG/ZB has the lowest COE of USD0.090 per kWh. In other words, the optimal configuration obtained is SPP(200 kW)/DG(82 kW)/ZB(2000 kWh), with cycle charging dispatch strategy. The initial cost of this configuration is USD163,445, and the operating cost is USD534 per year. These cost components are presented in Table 7.

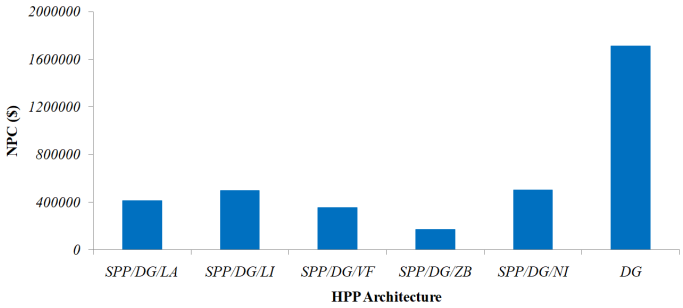

Figure 11. Comparison of the NPC of feasible architectures.

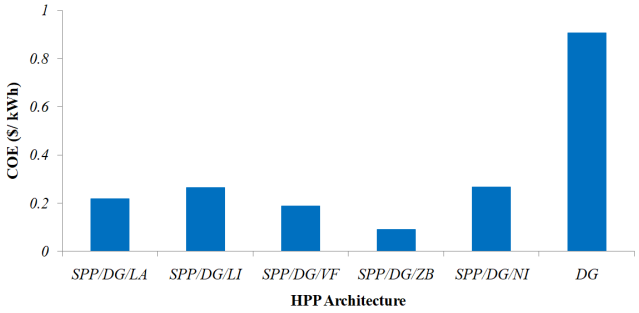

Figure 12. Comparison of the COE of feasible architectures.

6.2. Economic Analysis of Proposed Smart HPP with Different Battery Technologies

The optimal configuration for the selected load is SPP/DG/ZB. The other BSS technologies were compared with this optimal configuration obtained. Different cost components—capital cost, replacement cost, operations and maintenance (O&M) cost, fuel cost and salvage cost—are compared in Figure 13. The highest total cost is USD504,114 for SPP/DG/NI, and the lowest is USD170,396 for SPP/DG/ZB. SPP/DG/LI has the highest replacement cost of 26.8%, and SPP/DG/NI has the lowest replacement cost of 1.04%. O&M cost for SPP/DG/NI is the highest, at 17.6% of the total cost, and that of SPP/DG/ZB is the lowest, at 6.45% of the total cost. The fuel cost for the DG is the highest for SPP/DG/NI, at 9.7% of the total cost, and the lowest for SPP/DG/ZB is 0.95% of the total cost. Another relevant cost component is the system's value at the end of the useful life of the HPP component. This is known as salvage value. While determining the total cost of the HPP, this salvage value of HPP components is deducted. The salvage value for SPP/DG/NI is 11.3%, which is the highest, and that of SPP/DG/LA is 1.5%, which is the lowest. From this economic analysis, it has been observed that the highest total system cost is obtained for SPP/DG/NI, while the lowest is obtained for SPP/DG/ZB, which is taken as the optimal configuration for the selected load.

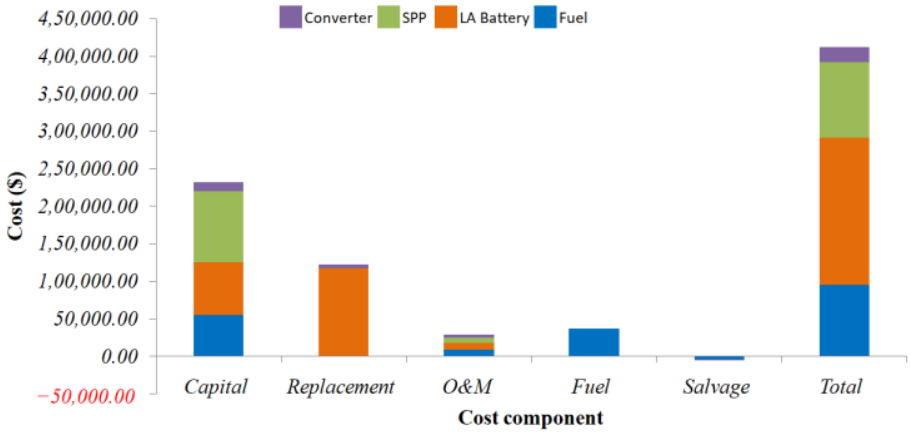

(**a**)

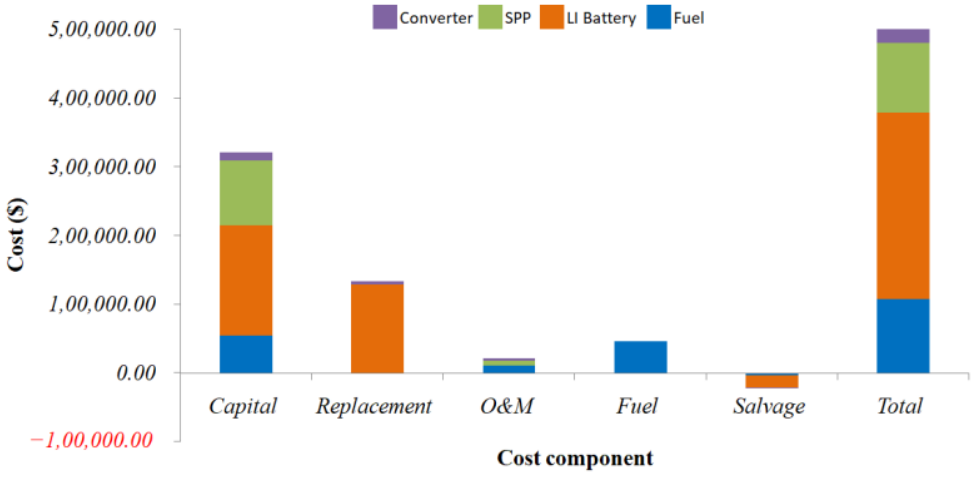

(**b**)

Figure 13. *Cont.*

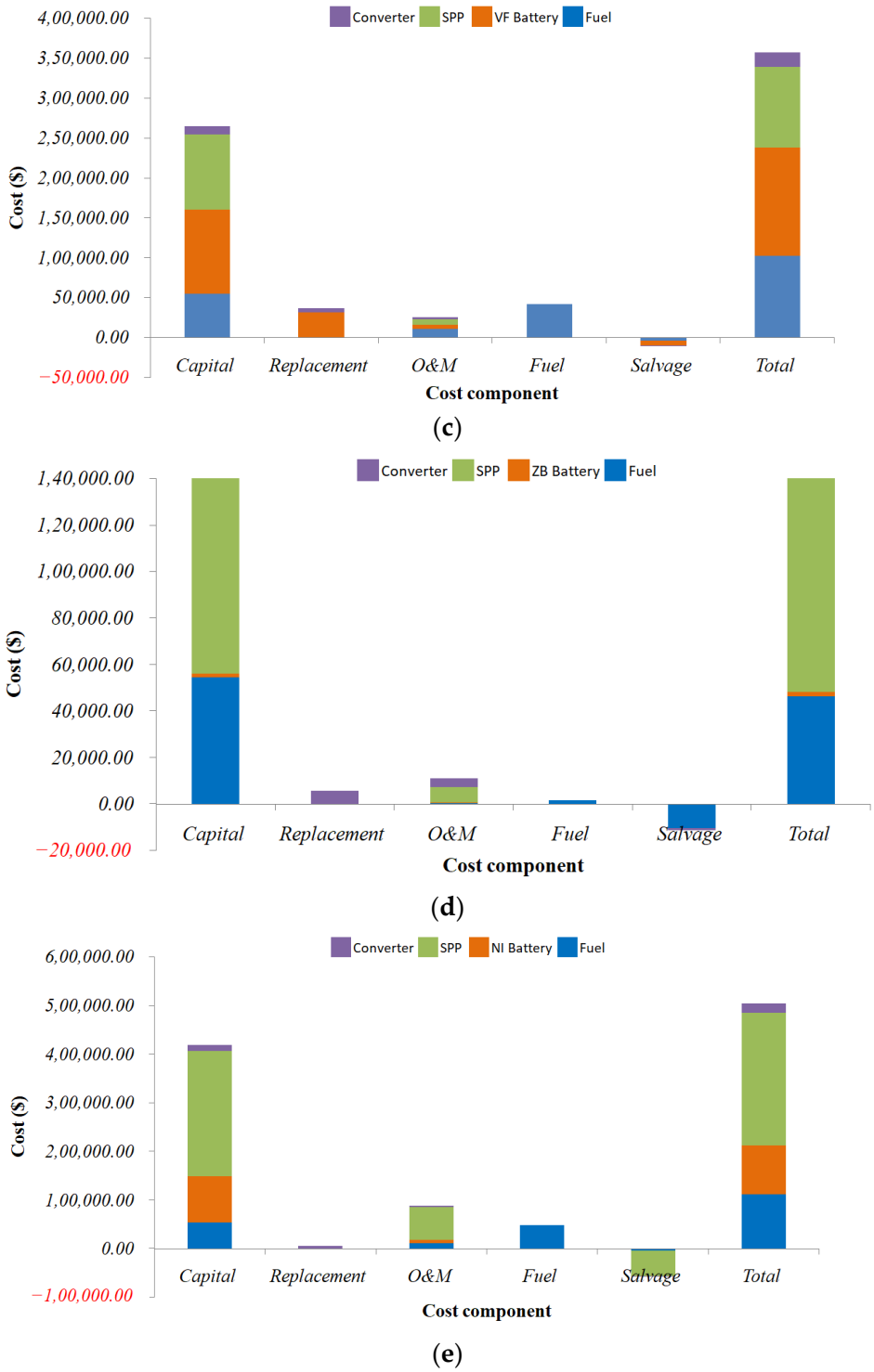

Figure 13. Summary of cost components of the HPP with configurations (**a**) SPP/DG/LA, (**b**) SPP/DG/LI, (**c**) SPP/DG/VF, (**d**) SPP/DG/ZB and (**e**) SPP/DG/NI.

The return on investment and simple payback period have also been considered for comparing the economics of the SPP/DG/LA, SPP/DG/LI, SPP/DG/VF, SPP/DG/ZB and SPP/DG/NI configurations of the HPP for the selected load in the current study. The graph shown in Figure 14 illustrates that the SPP/DG/ZB configuration has the highest return on investment, with the minimum time for the simple payback period.

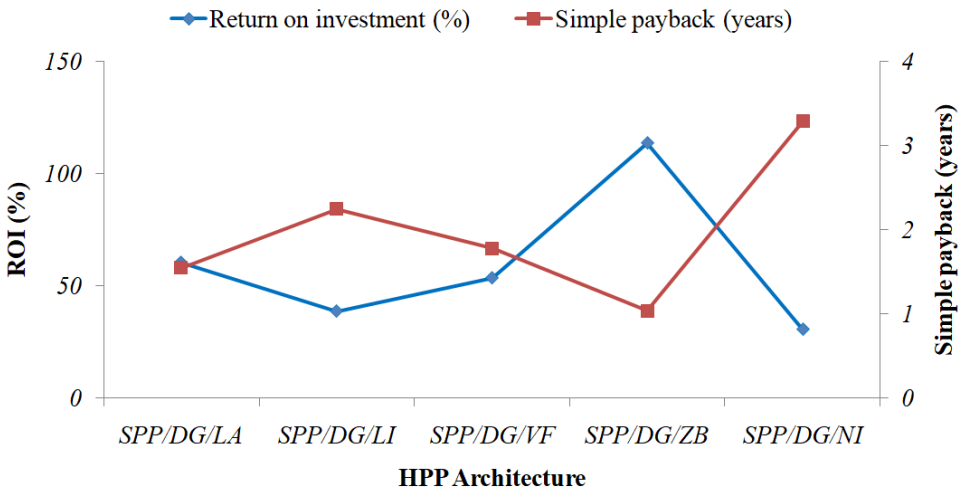

Figure 14. Comparison of ROI and simple payback period of the HPP with different BSS technologies.

6.3. Electricity Production with Different BSS Technologies

The average monthly electricity produced by the SPP/DG/BSS configuration using different BSS technologies—LA battery, LI battery, VF battery, ZB battery and NI battery—is shown in Figure 15. It was observed that the highest electricity generation was achieved in March and October. In these months, maximum electricity generation was obtained through SPP/DG/LI and SPP/DG/NI and the minimum by SPP/DG/ZB. In July, the lowest electricity generation was obtained. During this month, maximum electricity generation was obtained through SPP/DG/VF and SPP/DG/NI and the minimum by SPP/DG/ZB. The estimated average electricity generated by SPP/DG/LA, SPP/DG/LI, SPP/DG/VF, SPP/DG/ZB and SPP/DG/NI is 10,032 kW, 10,088 kW, 10,063 kW, 9830 kW and 10,106 kW, respectively.

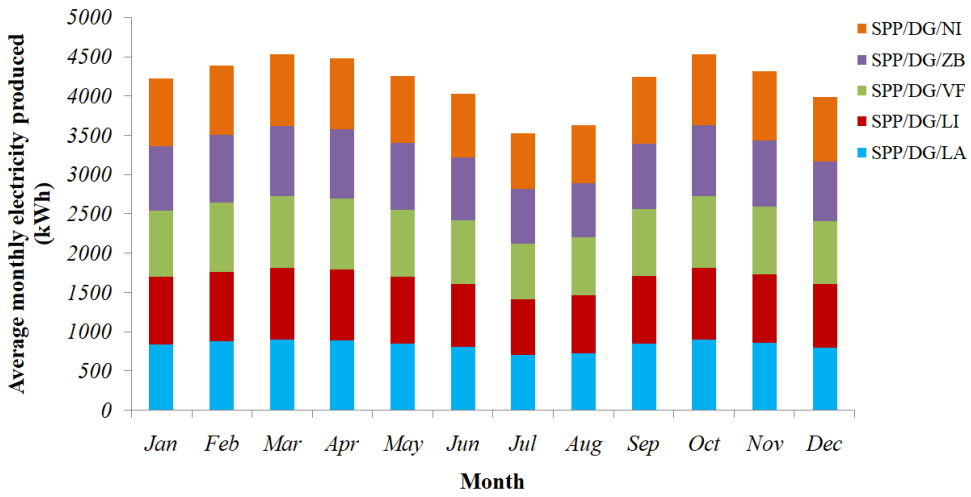

Figure 15. Average monthly electricity produced by SPP/DG/BSS using different BSS technologies.

6.4. Emissions of Pollutants with Different BSS Technologies

It is a matter of environmental concern to reduce the pollutant emissions in the atmosphere during the operation of the smart HPP to reduce its hazardous impact on life on Earth. This is mainly the operation of the DG in the HPP, as the burning of diesel causes air pollution. The emissions include harmful gases such as CO_2, carbon monoxide (CO), unburned hydrocarbons, particulate matter, sulfur dioxide (SO_2) and nitrogen oxide (NO_X). Table 8 compares pollutants emitted from the HPP with different BSS configurations. Simu-

lation by HOMER estimated that maximum fuel would be consumed by the SPP/DG/NI configuration. It is estimated that 8643 kg/year of CO_2 may be emitted. In contrast, the SPP/DG/ZB configuration may operate the DG the minimum number of times, and so the consumption of diesel may be the lowest. It is estimated that 288 kg/year of CO_2 may be emitted from the SPP/DG/ZB configuration.

Table 8. Emission of pollution from different HPP configurations.

HPP Configuration	CO_2 (kg/Year)	CO (kg/Year)	Unburned Hydrocarbons (kg/Year)	Particulate Matter (kg/Year)	SO_2 (kg/Year)	NO_X (kg/Year)
SPP/DG/LA	6439	40.6	1.77	0.246	15.8	38.1
SPP/DG/LI	8122	51.2	2.23	0.31	19.9	48.1
SPP/DG/VF	7360	46.4	2.02	0.281	18	43.6
SPP/DG/ZB	288	1.81	0.0792	0.011	0.705	1.7
SPP/DG/NI	8643	54.5	2.38	0.33	21.2	51.2
DG	194,038	1223	53.4	7.41	475	1149

6.5. Renewable Fraction in Smart HPP with Different BSS Technologies

The renewable source of energy in the current study is solar energy. Consequently, the ratio of electricity produced using the SPP to the total electrical load served gives the renewable fraction in the HPP. The renewable fraction of the selected BSS technologies is comparable, as presented in Table 9. The minimum renewable fraction is from SPP/DG/LI and SPP/DG/NI, 94%, and the maximum is provided by SPP/DG/ZB, 99%. It is estimated that the maximum renewable penetration in the SPP/DG/ZB configuration may be due to the high utilization of the energy generated by the SPP, and during night hours when the SPP is unable to serve the load, the ZB battery discharge may be able to fulfill the load demand. The DG may be operated the least for this configuration in such a case. Therefore, the SPP/DG/ZB configuration would be able to serve the load with clean energy and the minimum emission of pollutants in the atmosphere.

Table 9. Renewable fraction using different BSS technologies.

HPP Architecture	Renewable Production with Respect to Load (%)	Renewable Production with Respect to Generation (%)	Renewable Fraction (%)
SPP/DG/LA	204	97.9	96
SPP/DG/LI	204	97.3	94
SPP/DG/VF	204	97.6	95
SPP/DG/ZB	204	99.9	99
SPP/DG/NI	204	97.2	94

6.6. Performance of Different BSS Technologies

The performance of different BSS technologies used in the proposed smart HPP is compared in Table 10. This comparison was made on six parameters: energy in, energy out, storage depletion, losses, annual throughput and average energy cost. The total energy used for charging the battery bank is measured as 'energy in' in kWh per year. The minimum value of 'energy in' was obtained for the LI battery (82,164 kWh/year) and the maximum for the LA battery (93,467 kWh/year). In other words, the 'energy in' for the LI battery is 12.1% less than that for the LA battery. The energy discharged from the battery bank is measured as 'energy out' in kWh per year. The minimum value of 'energy out' was obtained for the NI battery (73,741 kWh/year) and the maximum for the ZB battery (79,287 kWh/year). In other words, the 'energy out' for the NI battery is 7% less than that for the ZB battery. It can be observed from Table 10 that due to various losses in the battery, 'energy out' is lower than 'energy in'.

Table 10. Performance parameters of different BSS technologies used in the HPP.

Performance Parameter	HPP Configuration				
	SPP/DG/LA	SPP/DG/LI	SPP/DG/VF	SPP/DG/ZB	SPP/DG/NI
Energy In (kWh/year)	93,467	82,164	92,050	87,858	86,544
Energy Out (kWh/year)	74,988	74,124	73,826	79,287	73,741
Storage Depletion (kWh/year)	240	186	−164	227	194
Losses (kWh/year)	18,719	8226	18,060	8797	12,997
Annual Throughput(kWh/year)	83,840	78,133	82,540	83,576	79,983
Average Energy Cost (USD/kWh)	0	0	0	0	0

The SOC level of the battery is affected by charging–discharging cycles of the BSS. The difference in the SOC level at the start and end of the year is measured as storage depletion. The minimum value of storage depletion was obtained for the VF battery (−164 kWh/year) and the maximum value for the LA battery (240 kWh/year). The SOC status for the ZB battery for a year is shown in Figure 16.

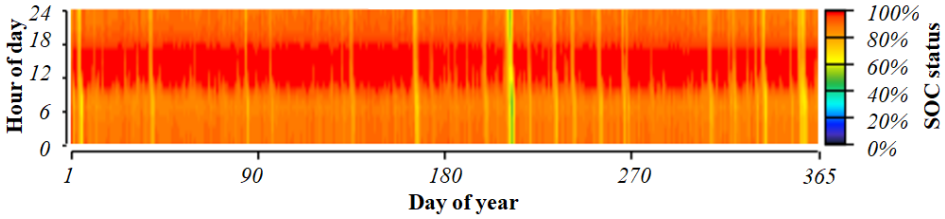

Figure 16. SOC status of the ZB battery in a year.

The losses in the BSS are due to power conversions and parasitic loads such as electronics, heating and cooling. The highest losses can be observed for the LA battery (18,719 kWh/year), and the lowest can be observed for the LI battery (8226 kWh/year). Annual throughput is the total energy cycled through the BSS in a year. The highest throughput was obtained for the LA battery (83,840 kWh/year) and the lowest for the LI battery (78,133 kWh/year). The average energy cost reflects the cost of deliberately charging the BSS. This is also known as storage energy cost. If the excess electricity generated is used to charge the BSS, then no storage cost is incurred. In an off-grid smart HPP, if the DG is operated to produce more electricity to charge the BSS, then storage energy cost is incurred. In the current study, the selected BSS technologies have no storage energy cost.

7. Sensitivity Analysis

It is relevant to perform a what-if analysis, also known as a sensitivity analysis, before commissioning a smart HPP. This analysis helps to study the impact of different parameters, which may affect the economics of the HPP. With the economic model provided by sensitivity analysis, the impact of one parameter on another can be estimated. In the current study, from the optimization result obtained from HOMER, SPP/DG/ZB is the optimal configuration for the proposed smart HPP. Sensitivity analysis was performed for this optimal configuration between BSS size and SPP size, with variables such as (1) BSS nominal capacity and COE and (2) renewable fraction and COE.

In Figure 17, the optimization variables were taken as the size of the SPP and BSS, with the CC dispatch control strategy. The sensitivity variable was considered as the ZB battery nominal capacity, and respective COE values were superimposed on the plot. The lowest COE was obtained as USD0.090 per kWh for two strings of ZB battery and 2000 kWh of nominal capacity. In Figure 18, the optimization variables are the same as taken for Figure 17, but the sensitivity variable considered here is the renewable fraction with COE values superimposed on it. It can be observed in the plot of Figure 18 that the points of lowest COE lay in the area with a renewable fraction of nearly 100%.

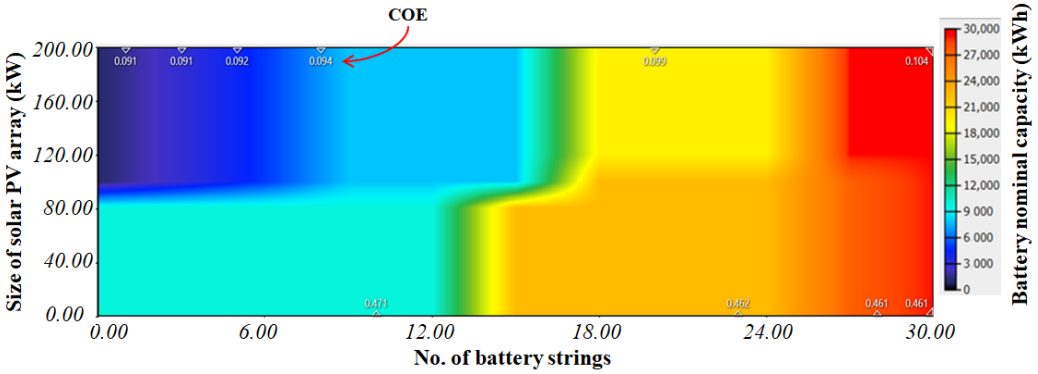

Figure 17. Variation in BSS nominal capacity with respect to BSS size and SPP size.

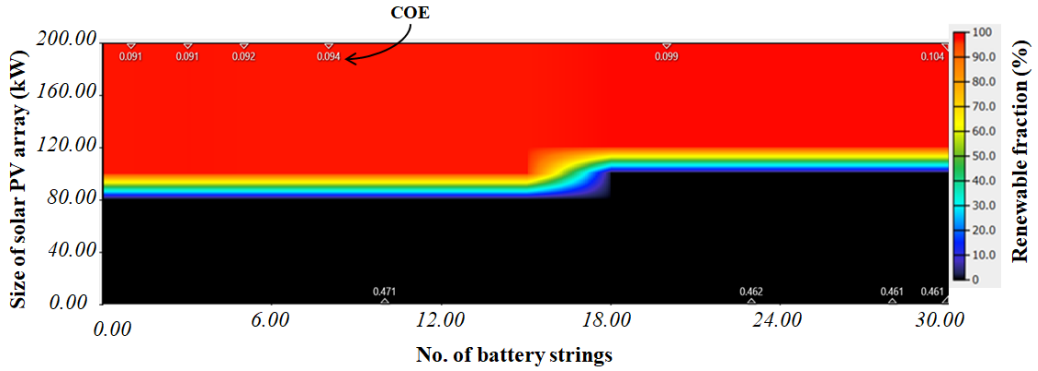

Figure 18. Variation in renewable fraction with respect to BSS size and SPP size.

8. Energy Balance

The optimal configuration for the proposed smart HPP was taken as SPP(200 kW)/DG (82 kW)/ZB(2000 kWh). To validate the optimal operation of this configuration, a time series analysis for a 24 h duration was conducted on the 2nd day of January. The individual contributions of the SPP, DG and BSS were plotted, along with the total electrical load served. The energy exchange outline between different power sources and load can be observed in Figure 19.

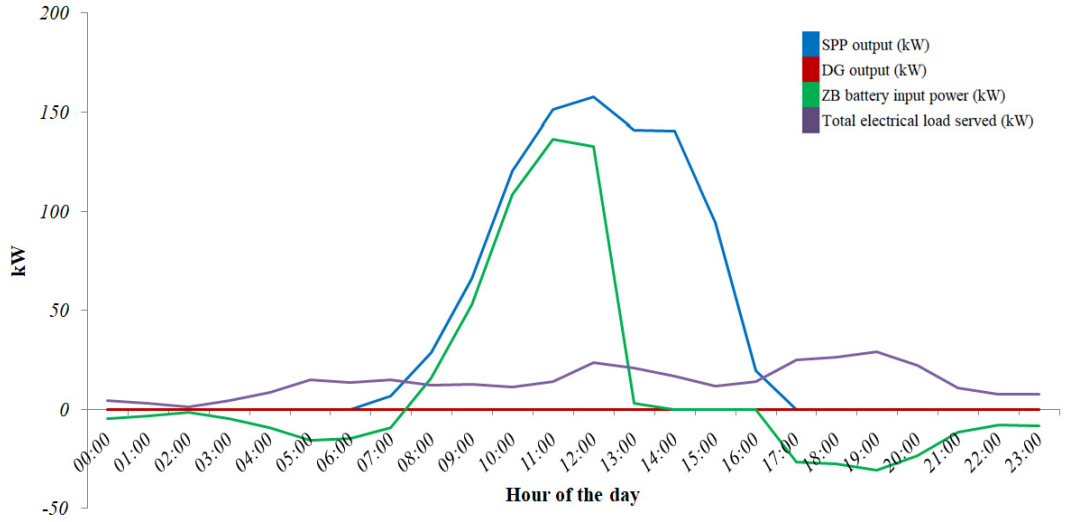

Figure 19. Time series analysis for 24 h operation of the HPP on the 2nd day of January.

1. From 0 to 6th hours—as the electricity demand was zero or minimum, the energy stored in the ZB battery served the load.
2. From 6th to 17th hours—the main producer of electricity is the SPP during the daytime. The SPP serves the load as well as charges the BSS with excess electricity produced.
3. From 17th to 23rd hours—as the electricity demand decreases in this duration, the energy stored in the ZB battery is enough to serve the load.
4. It is worthwhile to note that the DG was not required to generate power for the considered time, as electricity generated from the SPP was able to serve the load.

To verify the energy balance, we considered the values at the 11th hour of the day. The calculation for this time instant is presented in Table 11. It can be observed that the total generated electricity is equal to the total consumed electricity.

Table 11. Energy balance calculation from the time series plot.

Electricity Generation		Electricity Consumption	
SPP output	150 kW	ZB battery input power	136 kW
DG output	0 kW	Total electrical load served	14 kW
Total generation	150 kW	Total consumption	150 kW

9. Conclusions

This work intends to provide an optimal solution to generate electricity for a part of SRM IST, Delhi-NCR campus. The criteria for optimal solutions are to have a low cost of energy as compared to tariffs generated from the primary grid and to reduce the emission of pollutants into the atmosphere. The SPP/DG configuration analysis was conducted with different battery technologies using the HOMER Pro software. The optimal solution obtained is SPP(200 kW)/DG(82 kW)/ZB(2000 kWh), with cycle charging dispatch strategy. The analysis was based on initial cost, simple payback period, return on investment, energy produced, renewable penetration and emission of air pollutants. The following conclusions were drawn regarding this work:

1. The configuration of the proposed smart HPP had an SPP of 200 kW, DG of 82 kW, BSS with a nominal capacity of 2000 kWh and a converter of 68 kW.
2. The proposed smart HPP's initial cost is estimated at USD163,445 and the operating cost at USD534 per year.
3. The net present cost of the proposed smart HPP is estimated at USD170,348, and the estimated energy cost is USD0.090 per kWh.
4. It is estimated that on commissioning the proposed smart HPP, the emission of pollutants is expected to be reduced by 99.85%, from 194,038 kg/year to 288 kg/year.
5. Sensitivity analysis was performed by varying battery nominal capacity and renewable fraction. The size of the solar PV array and size of the battery were analyzed by these sensitivity variables.

In future, the analysis can be further modified by considering the government policies, subsidies provided by the government and related tariffs. The three major players—governments, utility companies and the energy sector—are expected to implement transparent procedures/policies to develop the renewable sector.

Author Contributions: Resources, R.C., G.F. and V.V.; supervision, H.S., V.B. and P.K.; writing—original draft, S.S.; writing—review and editing, H.S., V.B. and P.K. All authors have read and agreed to the published version of the manuscript.

Funding: This research received no external funding.

Institutional Review Board Statement: Not applicable.

Informed Consent Statement: Not applicable.

Data Availability Statement: The authors confirm that all data have been presented.

Conflicts of Interest: The authors declare no conflict of interest.

References

1. CO_2 Emissions. Available online: https://www.iea.org/reports/global-energy-review-2021/co2-emissions (accessed on 20 October 2022).
2. State of the Climate. Available online: https://www.unep.org/explore-topics/climate-action/ (accessed on 20 October 2022).
3. A Step towards Achieving India's Long Term Goal of Reaching Net-Zero by 2070. Available online: https://pib.gov.in/PressReleaseIframePage.aspx (accessed on 23 October 2022).
4. EU Economy Greenhouse Gases Still Below Pre-COVID Levels. Available online: https://ec.europa.eu/eurostat/web/products-eurostat-news/ (accessed on 20 October 2022).
5. Okonkwo, P.C.; Barhoumi, E.M.; Emori, W.; Shammas, M.I.; Uzoma, P.C.; Mohamed, A.M.A.; Abdullah, A.M. Economic evaluation of hybrid electrical systems for rural electrification: A case study of a rural community in Nigeria. *Int. J. Green Energy* **2022**, *19*, 1059–1071. [CrossRef]
6. Palit, D.; Kumar, A. Drivers and barriers to rural electrification in India—A multi-stakeholder analysis. *Renew. Sustain. Energy Rev.* **2022**, *166*, 112663. [CrossRef]
7. Renewable Energy. Available online: https://www.investindia.gov.in/sector/renewable-energy (accessed on 31 October 2022).
8. Power Sector at a Glance All India. Available online: https://powermin.gov.in/en/content/power-sector-glance-all-india (accessed on 31 October 2022).
9. Oosthuizen, A.M.; Inglesi-Lotz, R.; Thopil, G.A. The relationship between renewable energy and retail electricity prices: Panel evidence from OECD countries. *Energy* **2022**, *238*, 121790. [CrossRef]
10. List of Solar Power Plants/Solar Parks in India. Available online: https://www.jagranjosh.com/general-knowledge/list-of-solar-power-plants-in-india-1607686203-1 (accessed on 1 November 2022).
11. Sambhi, S.; Sharma, H.; Kumar, P.; Fotis, G.; Vita, V.; Ekonomou, L. Techno-Economic Optimization of an Off-Grid Hybrid Power Generation for SRM IST, Delhi-NCR Campus. *Energies* **2022**, *15*, 7880. [CrossRef]
12. Mayer, M.J.; Yang, D. Probabilistic photo-voltaic power forecasting using a calibrated ensemble of model chains. *Renew. Sustain. Energy Rev.* **2022**, *168*, 112821. [CrossRef]
13. Mayfield, B.; Tan, J.M.; Nazaripouya, H. Challenges and Advantages of Zinc Bromide Flow Batteries in Power System Applications. In Proceedings of the 2022 IEEE Kansas Power and Energy Conference (KPEC), Manhattan, KS, USA, 25–26 April 2022; pp. 1–5. [CrossRef]
14. Babaei, R.; Ting, D.S.-K.; Carriveau, R. Feasibility and optimal sizing analysis of stand-alone hybrid energy systems coupled with various battery technologies: A case study of Pelee Island. *Energy Rep.* **2022**, *8*, 4747–4762. [CrossRef]
15. Sambhi, S.; Sambhi, S.; Bhadoria, V.S. IoT based optimized and secured ecosystem for energy internet: The state of the art. In *Internet of Things in Business Transformation: Developing an Engineering and Business Strategy for Industry 5.0*; Scrivener Publishing LLC: Beverly, MA, USA, 2021; pp. 91–126. [CrossRef]
16. Qi, X.; Wang, J.; Królczyk, G.; Gardoni, P.; Li, Z. Sustainability analysis of a hybrid renewable power system with battery storage for islands application. *J. Energy Storage* **2022**, *50*, 104682. [CrossRef]
17. Kumar, P.; Pal, N.; Sharma, H. Techno-economic analysis of solar photo-voltaic/diesel generator hybrid system using different energy storage technologies for isolated islands of India. *J. Energy Storage* **2021**, *41*, 102965. [CrossRef]
18. Kordesch, K. Electrochemical Energy Storage. In *Energy Storage*; Silverman, J., Ed.; Pergamon: Oxford, UK, 1980; pp. 8–34. ISBN 9780080254715. [CrossRef]
19. Cole, W.; Frazier, A.W. Cost projections for utility- scale battery storage cost projections for utility- scale battery storage. *Natl. Renew Energy Lab* **2019**. NREL/ TP-6A20-73222. Available online: https://www.nrel.gov (accessed on 20 October 2022).
20. Salkuti, S.R. Energy storage technologies for smart grid: A comprehensive review. *Majlesi. J. Electr. Eng.* **2020**, *14*, 39–48.
21. Karampelas, P.; Ekonomou, L.; Fotis, G.; Vita, V. Evaluation of the Optimal Number of Wind Turbines in a Wind Farm Using the Downhill Simplex Optimization Method. *Int. J. Power Syst. Optim.* **2011**, *3*, 11–14.
22. Bnef, A. Behind the Scenes Take on Lithium-Ion Battery Prices. Available online: https://about.bnef.com/blog/behind-scenes-take-lithium-ion-battery-prices/ (accessed on 3 November 2022).
23. Ekonomou, L.; Fotis, G.; Vita, V.; Mladenov, V. Distributed Generation Islanding Effect on Distribution Networks and End User Loads Using the Master-Slave Islanding Method. *J. Power Energy Eng.* **2016**, *4*, 1–24. [CrossRef]
24. Sánchez-Díez, E.; Ventosa, E.; Guarnieri, M.; Trovò, A.; Flox, C.; Marcilla, R.; Soavi, F.; Mazur, P.; Aranzabe, E.; Ferret, R. Redox flow batteries: Status and perspective towards sustainable stationary energy storage. *J. Power Sources* **2021**, *481*, 228804. [CrossRef]
25. Samy, M.; Emam, A.; Tag-Eldin, E.; Barakat, S. Exploring energy storage methods for grid-connected clean power plants in case of repetitive outages. *J. Energy Storage* **2022**, *54*, 105307. [CrossRef]
26. Kreishan, M.Z.; Fotis, G.; Vita, V.; Ekonomou, L. Distributed Generation Islanding Effect on Distribution Networks and End User Loads Using the Load Sharing Islanding Method. *Energies* **2016**, *9*, 956. Available online: https://www.mdpi.com/1996-1073/9/11/956 (accessed on 20 October 2022). [CrossRef]
27. Kumar, P.P.; Saini, R.P. Optimization of an off-grid integrated hybrid renewable energy system with different battery technologies for rural electrification in India. *J. Energy Storage* **2020**, *32*, 101912. [CrossRef]

28. Bonkile, M.P.; Ramadesigan, V. Effects of sizing on battery life and generation cost in PV–wind battery hybrid systems. *J. Clean. Prod.* **2022**, *340*, 130341. [CrossRef]
29. Román, V.B.; Baños, G.E.; Solís, C.Q.; Flota-Bañuelos, M.; Rivero, M.; Soberanis, M.E. Comparative study on the cost of hybrid energy and energy storage systems in remote rural communities near Yucatan, Mexico. *Appl. Energy* **2022**, *308*, 118334. [CrossRef]
30. Das, B.K.; Hassan, R.; Islam, S.; Rezaei, M. Influence of energy management strategies and storage devices on the techno-enviro-economic optimization of hybrid energy systems: A case study in Western Australia. *J. Energy Storage* **2022**, *51*, 104239. [CrossRef]
31. Ganjei, N.; Zishan, F.; Alayi, R.; Samadi, H.; Jahangiri, M.; Kumar, R.; Mohammadian, A. Designing and Sensitivity Analysis of an Off-Grid Hybrid Wind-Solar Power Plant with Diesel Generator and Battery Backup for the Rural Area in Iran. *J. Eng.* **2022**, *2022*, 4966761. [CrossRef]
32. El-Houari, H.; Allouhi, A.; Salameh, T.; Kousksou, T.; Jamil, A.; El Amrani, B. Energy, Economic, Environment (3E) analysis of WT-PV-Battery autonomous hybrid power plants in climatically varying regions. *Sustain. Energy Technol. Assess.* **2021**, *43*, 100961. [CrossRef]
33. Nesamalar, J.J.D.; Suruthi, S.; Raja, S.C.; Tamilarasu, K. Techno-economic analysis of both on-grid and off-grid hybrid energy system with sensitivity analysis for an educational institution. *Energy Convers. Manag.* **2021**, *239*, 114188. [CrossRef]
34. Barelli, L.; Bidini, G.; Ciupageanu, D.; Pelosi, D. Integrating Hybrid Energy Storage System on a Wind Generator to enhance grid safety and stability: A Levelized Cost of Electricity analysis. *J. Energy Storage* **2021**, *34*, 102050. [CrossRef]
35. Malik, P.; Awasthi, M.; Sinha, S. Techno-economic and environmental analysis of biomass-based hybrid energy systems: A case study of a Western Himalayan state in India. *Sustain. Energy Technol. Assess.* **2021**, *45*, 101189. [CrossRef]
36. Google Maps. Available online: https://maps.google.com (accessed on 10 September 2022).
37. Why Despite Touching 1 Degree Celsius in Delhi, Mercury Won't Touch Zero-Mark. Available online: https://www.indiatoday.in/cities/delhi/story/delhi-sees-record-winter-temperature-drop-imd-1759412-2021-01-15 (accessed on 16 October 2022).
38. National Portal of India. Available online: https://www.india.gov.in/india-glance/profile (accessed on 17 October 2022).
39. Ghaithi, H.M.; Fotis, G.; Vita, V. Techno-Economic Assessment of Hybrid Energy Off-Grid System—A Case Study for Masirah Island in Oman. *Int. J. Power Energy Res.* **2017**, *11*, 103–116. [CrossRef]
40. Hotspots of Solar Potential in India. Available online: https://wgbis.ces.iisc.ernet.in/energy/paper/hotspots_solar_potential/results (accessed on 13 November 2022).
41. Solar Energy. Available online: https://mnre.gov.in/solar/current-status/ (accessed on 13 November 2022).
42. Jaiswal, S.P.; Bhadoria, V.S.; Singh, R.; Shrivastava, V.; Ambikapathy, A. Case Study on Modernization of a Micro-Grid and Its Performance Analysis Employing Solar PV Units. In *Energy Harvesting*; Enabling IOT Transformations, Chapman and Hall/CRC: Boca Raton, FL, USA, 2018; ISBN 9781003218760.
43. Bhadoria, V.S.; Pachauri, R.; Tiwari, S.; Jaiswal, S.; Alhelou, H.H. Investigation of Different BPD Placement Topologies for Shaded Modules in a Series-Parallel Configured PV Array. *IEEE Access* **2020**, *8*, 216911–216921. [CrossRef]
44. HOMER Pro 3.15. Available online: https://www.homerenergy.com/products/pro/docs/latest/index.html (accessed on 15 September 2022).
45. HOMER Software. Available online: www.homerenergy.com (accessed on 20 February 2021).
46. Solar Resource Glossary. Available online: https://www.nrel.gov/grid/solar-resource/solar-glossary.html (accessed on 20 February 2021).
47. Direct Solar Irradiation. Available online: https://www.sciencedirect.com/topics/engineering/direct-normal-irradiation (accessed on 20 February 2021).
48. NASA Power—Data Access Viewer. Available online: https://power.larc.nasa.gov/data-access-viewer/ (accessed on 10 February 2021).
49. Adewumi, O.B.; Fotis, G.; Vita, V.; Nankoo, D.; Ekonomou, L. The Impact of Distributed Energy Storage on Distribution and Transmission Networks' Power Quality. *Appl. Sci.* **2022**, *12*, 6466. [CrossRef]
50. Fotis, G.; Dikeakos, C.; Zafeiropoulos, E.; Pappas, S.; Vita, V. Scalability and Replicability for Smart Grid Innovation Projects and the Improvement of Renewable Energy Sources Exploitation: The FLEXITRANSTORE Case. *Energies* **2022**, *15*, 4519. [CrossRef]
51. Adefarati, T.; Bansal, R.C.; Justo, J.J. Techno-economic analysis of a PV–wind–battery–diesel stand-alone power system in a remote area. *J. Eng.* **2017**, *2017*, 740–744. [CrossRef]
52. Agyekum, E.B.; Nutakor, C. Feasibility study and economic analysis of stand-alone hybrid energy system for southern Ghana. *Sustain. Energy Technol. Assess.* **2020**, *39*, 100695. [CrossRef]
53. Zafeiropoulou, M.; Mentis, I.; Sijakovic, N.; Terzic, A.; Fotis, G.; Maris, T.I.; Vita, V.; Zoulias, E.; Ristic, V.; Ekonomou, L. Forecasting Transmission and Distribution System Flexibility Needs for Severe Weather Condition Resilience and Outage Management. *Appl. Sci.* **2022**, *12*, 7334. [CrossRef]
54. Li, C.; Zhou, D.; Wang, H.; Lu, Y.; Li, D. Techno-economic performance study of stand-alone wind/diesel/battery hybrid system with different battery technologies in the cold region of China. *Energy* **2020**, *192*, 116702. [CrossRef]
55. Das, B.K.; Hoque, N.; Mandal, S.; Pal, T.K.; Raihan, M.A. A techno-economic feasibility of a stand-alone hybrid power generation for remote area application in Bangladesh. *Energy* **2017**, *134*, 775–788. [CrossRef]
56. Kaur, M.; Dhundhara, S.; Verma, Y.P.; Chauhan, S. Techno-economic analysis of photovoltaic-biomass-based microgrid system for reliable rural electrification. *Int. Trans. Electr. Energy Syst.* **2020**, *30*, e12347. [CrossRef]
57. Kumar, P.; Pal, N.; Sharma, H. Performance analysis and evaluation of 10 kWp solar photo-voltaic array for remote islands of Andaman and Nicobar. *Sustain. Energy Technol. Assess.* **2020**, *42*, 100889.

58. Homer Energy. Available online: https://www.homerenergy.com/products/pro/docs/3.11/homers_calculations.html (accessed on 26 October 2022).
59. Sijakovic, N.; Terzic, A.; Fotis, G.; Mentis, I.; Zafeiropoulou, M.; Maris, T.I.; Zoulias, E.; Elias, C.; Ristic, V.; Vita, V. Active System Management Approach for Flexibility Services to the Greek Transmission and Distribution System. *Energies* **2022**, *15*, 6134. [CrossRef]
60. Hadjiionas, S.; Oikonomou, D.S.; Fotis, G.; Vita, V.; Ekonomou, L.; Pavlatos, C. Green Field planning of distribution systems. In Proceedings of the 11th WSEAS International Conference on Automatic Control, Modeling and Simulation (ACMOS 2009), Istanbul, Turkey, 30 May 30–1 June 2009; pp. 340–348.
61. Aziz, A.S.; Tajuddin, M.F.; Adzman, M.R.; Ramli, M.A.; Mekhilef, S. Energy management and optimization of a PV/diesel/battery hybrid energy system using a combined dispatch strategy. *Sustainability* **2019**, *11*, 683. [CrossRef]
62. Sambhi, S.; Sharma, H.; Bhadoria, V.; Kumar, P.; Chaurasia, R.; Chaurasia, G.S.; Fotis, G.; Vita, V.; Ekonomou, L.; Pavlatos, C. Economic Feasibility of a Renewable Integrated Hybrid Power Generation System for a Rural Village of Ladakh. *Energies* **2022**, *15*, 9126. [CrossRef]
63. Yadav, R.K.; Bhadoria, V.S.; Hrisheekesha, P. Technical and Financial Assessment of a Grid Connected Solar PV Net Metering System for Residential Community. In Proceedings of the 2019 2nd International Conference on Power Energy. Environment and Intelligent Control (PEEIC), Greater Noida, India, 18–19 October 2019; pp. 299–303. [CrossRef]